ELM Control by Resonant Magnetic Perturbations: Overview of Research by the PEP ITPA Group

M.E. Fenstermacher 1), M. Becoulet 2), P. Cahyna 3), J. Canik 4), C.S. Chang 5), T.E. Evans 6), P. Gohil 6), S. Kaye 7), A. Kirk 8), Y. Liang 9) 10)*, A. Loarte 11), R. Maingi 4), O. Schmitz 9), W. Suttrop 12), and H.R. Wilson 13)

1) Lawrence Livermore National Laboratory, PO Box 808, Livermore California 94551 USA
2) CEA/IRFM, 13108 St Paul-lez-Durance, France
3) Institute of Plasma Physics AS CR, Association EURATOM/IPP.CR Prague Czech Repub
4) Oak Ridge National Laboratory, Oak Ridge, Tennessee 37831, USA
5) Courant Institute of Mathematical Sciences, New York University, NY 10012, USA
6) General Atomics, P.O. Box 85608, San Diego, California 92186-5608, USA
7) Princeton Plasma Physics Laboratory, PO Box 451, Princeton, NJ 08543-0451, USA
8) EURATOM/CCFE Fusion Assn, Culham Science Cntr, Abingdon Oxon OX14 3DB UK
9) Forschungszentrum Jülich GmbH, Association EURATOM-FZ Jülich, Institut für Energieforschung-Plasmaphysik, Trilateral Euregio Cluster, D-52425 Jülich, Germany
10) JET-EFDA, Culham Science Centre, Abingdon, OX14 3DB , UK
11) ITER Organization, Route de Vinon sur Verdon, 13115 Saint Paul Lez Durance, France
12) Assoc. EURATOM-Max-Planck-Institut für Plasmaphysik, D-85748 Garching, Germany
13) University of York, Heslington, York YO10 5DD UK

e-mail contact of main author: fenstermacher@fusion.gat.com

Abstract. Modifications of edge localized modes (ELMs) with resonant magnetic perturbations (RMPs) in H-mode plasmas have been achieved in DIII-D, JET, JFT-2M MAST, NSTX and TEXTOR including (i) suppression of ELM energy losses with internal coils in DIII-D, (ii) mitigation of ELM size with external coils in JET and with internal coils in DIII-D, MAST and TEXTOR, and (iii) pacing of ELMs with modulated RMP pulses in NSTX and DIII-D. The experiments in DIII-D, JET, MAST and NSTX confirm that the island overlap width condition, correlated with ELM suppression in DIII-D and used to guide the design requirements of ITER RMP coils, is not sufficient to assure ELM suppression in multiple devices. They also indicate that the L-H threshold power increases when RMP fields of sufficient amplitude are applied during the L-mode phase of the discharges. For 2011 and beyond, upgrades of the internal RMP coil systems are underway at AUG, DIII-D, and MAST, and upgrades are under consideration at JET and NSTX, that will permit greater variation of RMP mode spectrum to test ELM control physics models. These systems will greatly increase the capability to test theoretical models of RMP ELM control and the probability of achieving ELM suppression on multiple tokamaks.

1. Introduction

This paper presents a multi-tokamak overview of experimental results and planned hardware upgrades that should ultimately provide the essential physics understanding needed to project results from present and future resonant magnetic perturbation (RMP) edge localized mode (ELM) control experiments in DIII-D [1-17], JET [18-25], MAST [26-28], NSTX [29-30], TEXTOR [31-33], JFT-2M [34], AUG [35], and COMPASS [36] to ITER [37]. Reduction of ELM size by at least a factor of 20 is critical to achieve acceptably low erosion of ITER material surfaces [38] for the baseline 15 MA scenario. The joint work reported here is part of the plan formulated by the ITPA Pedestal and Edge Physics (PEP) group and the ITER IO to provide the physics basis supporting the proposed use of internal RMP coils for ITER ELM control. In this plan, issues that need to be addressed for all ELM control schemes in ITER include: 1) control of the first ELM including during I_p ramp-up, 2) compatibility with high core and separatrix densities, low heat flux to the first wall, and high pedestal pressure at low collisionality, 3) minimal effect on the L-H threshold power, toroidal rotation, core MHD

and locked mode thresholds, and 4) for controlled ELMs, no detrimental effects on the balance of conductive vs. convective power, average ELM power, spatial heat flux deposition profiles and time scales. Issues for RMP ELM control in particular include: 1) whether a minimum edge island overlap width is sufficient to assure ELM suppression, 2) whether >20x reduction of target impulsive energy with controlled ELMs can be demonstrated, 3) the effect of plasma rotation on self-consistent fields within the plasmas (shielding or amplification of vacuum fields), 4) the level of target heat flux asymmetries introduced and the implied RMP toroidal rotation frequency needed to meet maximum steady heat flux limits, and 5) whether the RMP changes the between-ELM heat flux level or spatial structure. Joint work on these issues is formulated by the ITPA PEP group in terms of three multi-machine experiments: PEP-19 Basic Mechanisms of Edge Transport with RMPs in Toroidal Plasma Devices, PEP-23 Quantification of the Requirements for ELM Suppression by Magnetic Perturbations from Internal Off-Midplane Coils and PEP-25 Inter-machine Comparison of ELM Control by Magnetic Field Perturbations from Midplane RMP Coils. Experimental progress made on some of these issues will be presented below.

ELM characteristics have been modified by RMPs on many devices (Figs. 1 and 4). ELM mitigation, defined here as reduction of ELM size and increase of ELM frequency, has been demonstrated using static RMP fields of various toroidal mode numbers in JET [18-25], and in DIII-D [7,8,14,17], MAST [26-28], and TEXTOR [33]. ELM suppression, i.e. complete elimination of ELM heat flux transients in a plasma with good H-mode confinement, has been seen robustly on DIII-D using static n=3 fields in both high [1-4] and low collisionality [5-17] plasmas, but not yet on any other device. Finally, ELMs have been synchronized with modulated RMP pulses to frequencies higher than, and amplitudes lower than, the natural Type-I ELM characteristics (ELM pacing) on both NSTX [29-30] and DIII-D [39]. In the discussion below, results obtained with static RMP fields will be grouped together separately from results with modulated fields, since the engineering requirements for systems to produce the required fields could be significantly different.

2. Effects of DC Resonant Magnetic Perturbation Fields for ELM Control

Static RMP fields affect both the ELM characteristics and other performance properties of H-mode plasmas. Although the state of the plasma prior to, and its response to the application of, the RMP fields varies between the devices, some common observations are emerging regarding the change in ELM characteristics, the effects on pedestal density and the L-H threshold power, and the criteria used to guide the design of the ITER RMP coils, as discussed below.

2.1 ELM Characteristics Modified by RMPs

The response of ELMs, in single and double-null ELMing H-mode plasmas, to application of static RMP fields ranges from little observed change to significant mitigation and ELM suppression [1-28,31-34]. There are also cases of ELMs induced by application of RMP fields in otherwise transient ELM-free H-mode plasmas in NSTX [29-30], MAST [26-28] and JFT-2M [34]. Examples of key results showing modification of ELM characteristics in ELMing H-mode plasmas are given in Fig. 1. In the DIII-D case [Fig. 1(a)], ELM suppression is obtained in lower single-null (LSN) plasmas at low collisionality (low ν^*) using even parity (up/down symmetric) n=3 fields from internal, off-midplane coils for a particular value of

q_{95}~3.6 that aligns a peak in the n=3 vacuum RMP spectrum with the equilibrium field profile [6-8,12]. ELM suppression has also been obtained in similar plasmas with q_{95}~7.2 with up/down asymmetric RMP fields [8] that were pitch aligned with the equilibrium field at the higher q-value, supporting the hypothesis that RMP pitch resonance is important for ELM suppression. In the JET example [Fig. 1(b)], Type-I ELMs are mitigated in LSN, low ν* plasmas by n=1 fields from external, on-midplane coils [18-23]. This result is obtained over a large range of q_{95} suggesting that the ELM mitigation is not a narrowly defined resonant phenomenon. Type-I ELM mitigation has also been seen using n=2 fields from the external coils in JET [23-25] and with n=2 and n=3 fields from the internal, off-midplane coils in DIII-D when q_{95} is outside the resonant window for suppression [7,8]. In the JET case with both n=1 and n=2 fields, the ELM frequency data suggests multiple narrow resonances during q_{95} sweeps [25]. The maximum reduction factors of the size of the largest Type-I ELMs normalized to the plasma stored energy in the mitigation cases are at least 3.5x with n=1 fields in JET, ~2.5x with n=2 fields in JET, and ~2.3x with n=3 fields in DIII-D. Application of n=3 fields from internal off-midplane coils in double-null MAST plasmas at moderate collisionality [Fig. 1(c)] eventually, although not immediately at RMP turn-on, changes the ELMs from Type-I to small Type-IV [28]. Finally, ELM mitigation has been seen also in circular, limited TEXTOR H-mode plasmas [33] at high collisionality [Fig. 1(d)] using m/n=6/2 RMP fields from the centerpost helical Dynamic Ergodic Divertor (DED) coil. Note that each of these examples shows evidence of some reduction of plasma density (pumpout) when the ELMs are mitigated or suppressed. This is a common feature of ELM control by static RMP fields in H-mode plasmas [10,23,26,30,40]. Density pumpout is also seen when RMP fields are applied in some L-mode plasmas [26,31,40].

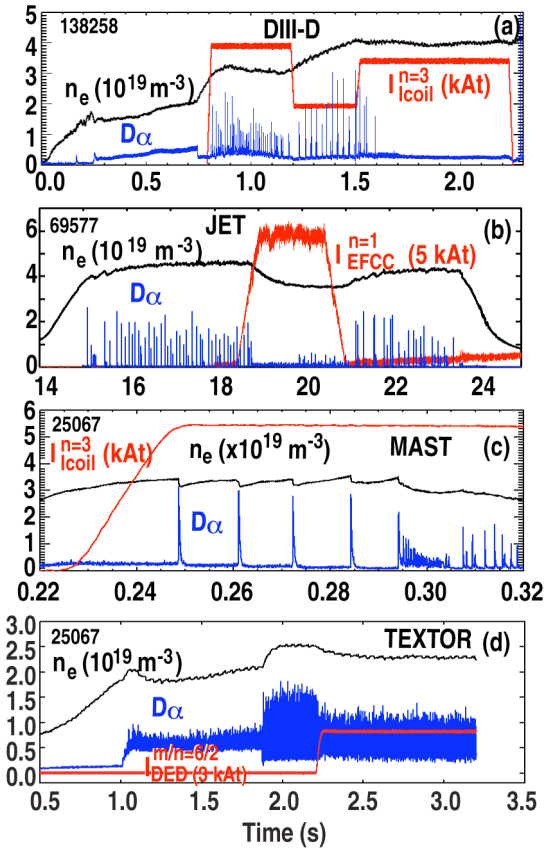

FIG. 1. Evolution of line averaged density (black), RMP coil current (red) and edge D_α emission (blue) during ELM control discharges using dc static RMP fields in (a) DIII-D, (b) JET, (c) MAST and (d) TEXTOR.

2.2 Effect of RMP on L-H Power Threshold

The threshold power to achieve the L-H transition is observed to be higher in DIII-D, MAST and NSTX plasmas with RMPs having strong resonant components in the spectrum, but less effect on $P_{L\text{-}H}$ was seen in DIII-D and MAST using RMPs with only weak resonant components. The L-H threshold power normalized to its value without RMP fields is shown as a function of the RMP perturbation strength in Fig. 2. Here RMP perturbation strength is parameterized by the width, in normalized poloidal flux, of the island overlap region where the Chirikov parameter (sum of island half widths normalized by island spacing) [41] exceeds

1.0 using the vacuum fields. This parameter was chosen in an attempt to allow comparison of results from experiments with significantly different operational parameters. The island overlap widths for all the devices were calculated using the same Fourier harmonics representation of the vacuum magnetic fields in the SURFMN code as used to guide the ITER RMP coils design [8,42]. The L-H threshold power is obtained in the experiments by applying the RMP fields during the L-mode phase of the discharge and then increasing the input beam power (by slow ramps in MAST and NSTX or by a series of steps in DIII-D) until the L-H transition is observed. For DIII-D cases with strong resonant components in the RMP spectrum (q_{95} within the resonant window for ELM suppression), the L-H power threshold shows little increase for small RMP fields, but significant increases for perturbations beyond a threshold amplitude [for details see Ref. 43]. Similar increases in $P_{L–H}$ are observed with strong resonant fields in MAST for perturbations larger than a threshold value. Strong perturbation fields that are off resonance (q_{95} outside the resonant window for ELM suppression) show little effect on P_{L-H} in DIII-D, but some effect in MAST for large overlap region width. These results suggest that P_{L-H} may only be affected when sufficient resonant perturbation (possibly more than needed for ELM suppression [8,11]) is applied. Further experiments are planned to solidify this result, and theoretical work is planned to give the physics understanding needed to extrapolate it with confidence to future devices including ITER.

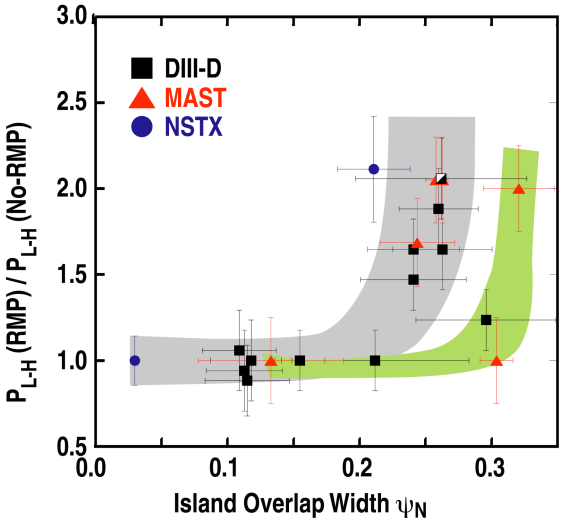

FIG. 2. Normalized L-H threshold power as a function of island overlap width using the vacuum fields showing data from DIII-D (black), MAST (red) and NSTX (blue). The applied RMP spectrum has strong resonant components for data points in the grey shaded region. The resonant components are much weaker than the non-resonant components in the RMP spectrum for points in the green shaded region.

2.3 Threshold Island Overlap Width Not Sufficient for ELM Suppression

Recent multi-machine experimental comparisons [26] show that one of the criteria guiding the design of the ITER RMP coils [42], i.e. that the RMP vacuum magnetic island overlap width $\Delta_{Chir>1}$ in the edge plasma be ≥ the threshold width correlated with ELM suppression in DIII-D [8, 11], may be necessary to achieve ELM suppression in ITER but it is not sufficient to assure ELM suppression. The database for this comparison has been expanded as part of the ITPA PEP RMP working group studies. Profiles of the Chirikov parameter as a function of normalized poloidal flux in the pedestal region calculated by the SURFMN code [42] are shown in Fig. 3 for H-mode discharges in DIII-D [8,11], JET [18-23], MAST [26-28] and NSTX [29-30]. The DIII-D cases (discharges #126440 and #131518) are examples of time slices during ELM suppression in which the island overlap region widths are equal to the threshold values ($\Delta_{Chir>1}$=0.165 and $\Delta_{Chir>1}$=0.132 respectively) determined from the databases reported in Refs. 8 and 11, respectively. Although several of the examples from discharges in other devices met or exceeded the guidance overlap width, none of the other cases in Fig. 3 obtained ELM suppression. Both of the cases with RMP from external, midplane coils in JET

(pulses #69557 with n=1 RMP and #75793 with n=2 RMP) showed significant ELM mitigation [20,23]. In the MAST case, the n=3 RMP from internal off-midplane coils produced the transition from large, infrequent Type-I ELMs to smaller, rapid Type-IV ELMs [as shown in Fig. 1(c)] [28]. Finally, in the NSTX case, application of the n=3 RMP from external, midplane coils triggered ELMs in an otherwise transient ELM-free H-mode plasma [29,30]. Clearly large island overlap width calculated from vacuum fields is not sufficient to assure ELM suppression across multiple devices. Further discussion is given in Sec. 4.

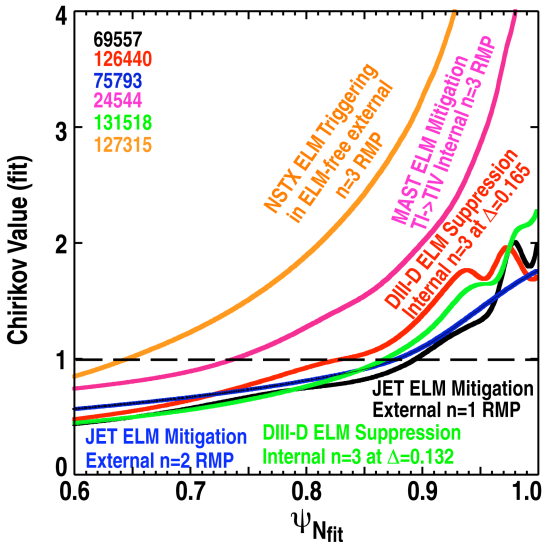

FIG. 3. Profiles of the Chirikov parameter as functions of normalized poloidal flux for H-mode discharges in DIII-D (red & magenta), JET (black & blue), MAST (green) and NSTX (orange). In the DIII-D cases Type-I ELMs are suppressed, in the JET cases the Type-I ELMs are mitigated, in the MAST case the RMP triggers a Type-I to Type-IV ELM transition, and in the NSTX case the RMP triggers ELMs in an evolving ELM-free plasma.

3. ELM Pacing Using Time Varying RMP Fields

Modulation of RMP amplitude has been used to control ELM frequency (pacing) and reduce ELM size at high paced ELM frequency in NSTX [29-30] and DIII-D [39] (Fig. 4). In NSTX, short (11 ms) square wave pulses of n=3 RMP from external midplane coils (vacuum vessel penetration e-folding time ~4 ms) are applied to otherwise transient ELM-free H-mode plasmas [Fig. 4(a)]. The normalized ELM energy loss as a function of the applied RMP pulse frequency (Fig. 5) shows a reduction of the mean size of the largest 20% of the ELMs by a factor of 2 when the pacing frequency is increased by a factor of 6. In DIII-D, sinusoidal n=3 RMP amplitude from the internal off-midplane coils was applied to otherwise steady ELMing H-mode plasmas [Fig. 4(b)]. At high collisionality the natural ELM frequency was low (~10 Hz) because the input

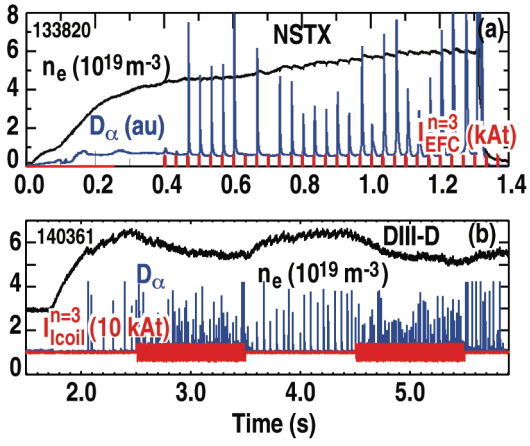

FIG. 4. Evolution of line averaged density (black), RMP coil current (red) and edge D_α emission (blue) for (a) NSTX plasma with ELMs paced by pulsed RMP fields, and (b) DIII-D plasma with ELMs paced by oscillatory RMP fields.

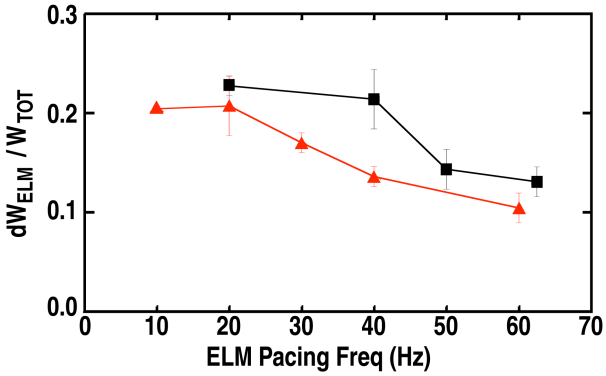

FIG. 5. Mean normalized energy loss of the largest 20% of ELMs as a function of ELM pacing frequency using square wave RMP pulses for NSTX H-mode plasmas at 1.0 MA (black squares) and 0.8 MA (red triangles).

power was near $P_{L\text{-}H}$. As the RMP frequency increased, the density decreased (evidence of pump-out) and the natural ELM frequency increased, consistent with typical behavior of Tyle-I ELMs when P_{inj} - $P_{L\text{-}H}$ is increased [Fig. 4(b)]. However, with the RMP, the higher frequency ELMs were synchronized to twice the applied RMP frequency. At low collisionality in DIII-D, the natural ELM frequency was high (~100 Hz). Full synchronization of the largest ELMs with twice the applied RMP frequency was obtained for frequencies near the natural ELM frequency, but for higher RMP frequency the synchronization fraction decreased. Although the experimental conditions were qualitatively different between DIII-D and NSTX, some common observations are obtained. In both cases the ELMs are 100% synchronized to the modulated fields for low modulation frequency but as the perturbation frequency increased the synchronization fraction decreased. For the range of frequencies with full synchronization, the reduction of ELM size was less than proportional to the increase in ELM frequency, suggesting that there may be a limit to the maximum ELM reduction even if full synchronization could be maintained. After periods in which the ELMs were not synchronized with the modulated fields, the next ELM was frequently larger than the previously synchronized ELMs.

4. Discussion

This paper presents some common observations from the current collection of qualitatively different RMP ELM control experiments in tokamaks. Some of the aspects of present experiments that must be investigated further in joint ITPA experiments include differences in: 1) plasma shape (SND vs DND, low vs high triangularity) and its effect on ELM instability during RMP, 2) plasma collisionality and its effect especially on the bootstrap current drive for ELM instability during RMP, 3) mix of resonant and non-resonant components in the RMP spectrum and 4) spatial profiles of the RMP fields within the plasma including the plasma response. Physics understanding of the effect of these parameters on RMP ELM control is needed for confident extrapolation of present results to ITER.

Although significant island overlap in the pedestal may be necessary to achieve ELM suppression, other aspects of RMP application could play important roles in assuring ELM suppression in multiple devices; quantification of overall design guidance criteria is still in progress. Empirically there are indications that the degree of pitch alignment of the RMP fields with the equilibrium confinement field and the plasma collisionality could be important. Also, the radial localization of the RMP fields in the pedestal region may be important, but detailed physics understanding of the radial profile of possible screening of the applied vacuum RMP fields by the plasma is also still under development [44 and references therein]. Formulating design guidance criteria for these and other aspects of RMP ELM control will continue to be a significant part of the ITPA PEP RMP group work.

5. Plans for Future RMP ELM Control Hardware and Experiments

The planned upgrades of the coil systems internal to the vacuum vessel on several devices (Fig. 6) will permit significantly greater variation of RMP mode spectrum to test physics models of RMP ELM control for experiments in 2011 and beyond. A new set of three rows of internal coils is proposed for the centerpost of DIII-D [Fig. 6(a)]. When used in combination with the present two rows of coils above and below the outer midplane, the centerpost coils would ultimately allow variation of the RMP radial and poloidal localization plus the

capability to separately rotate either n=3 or n=4 RMPs toroidally for tests of field penetration and heat flux spreading models. Work has been done to design and test prototype centerpost coils, but the time scale for the ultimate installation of the set of 36 coils is still under review. MAST will install 6 additional internal coils below the outer midplane [Fig. 6(b)], for a total of 12 in the lower row and 6 in the upper row, to increase the RMP spectral flexibility. These coils should be ready for experiments in 2011. In this same time frame experiments will begin at AUG with a new set of 4 internal coils above and 4 below the outer midplane [35], and at COMPASS with the existing n=2 coil set and a planned extension to n=4. Within a year the plan at AUG is to upgrade to 8 internal coils above, 8 below and 8 on the outer midplane [Fig. 6(c)] in a configuration similar to the ITER design. JET [45], NSTX [46], TCV [47] and JT60-SA [48] are currently engaged in studies of the feasibility of installing internal coils. The internal coils in KSTAR [49] can be used to produce RMPs. Taken together, these systems will greatly increase both the capability to test theoretical models of ELM control by RMP fields and the probability of achieving ELM suppression on multiple tokamaks worldwide.

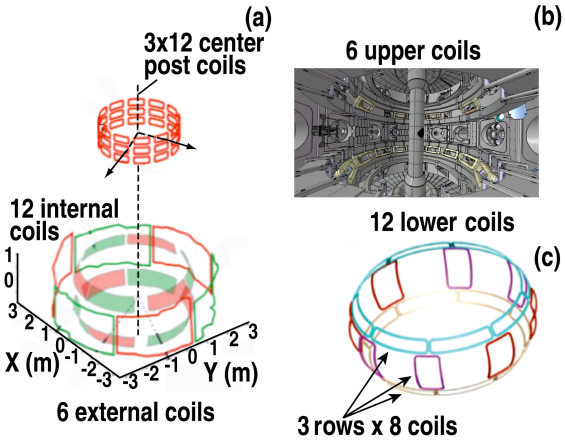

FIG. 6. Schematic diagrams of proposed new systems of internal coils for future RMP ELM control experiments in (a) DIII-D – ultimately 36 coils on the centerpost, (b) MAST – additional 6 coils in row below the midplane, and (c) ASDEX-Upgrade – ultimately 3 rows (above, below & on midplane) of 8 coils.

6. Summary and Conclusions

Recent experiments using RMPs in multiple tokamaks show modification of ELM characteristics for a variety of RMP spectral components and plasma conditions. Suppression of ELMs is seen robustly in DIII-D for a range of plasma conditions but only for a finite window of resonant values of the equilibrium field pitch angle in the pedestal region. Suppression of Type-I ELMs in an H-mode plasma has not been obtained on any other tokamak to date. Mitigation of ELM size by significant factors has been obtained in multiple tokamaks with a variety of RMP spectra in a wide range of plasma equilibria, but reduction of Type-I ELM size by a factor of 20 during RMP ELM mitigation without degradation of the H-mode confinement, as required for full power ITER operations, has not yet been obtained. Multi-machine data suggests that the threshold power for the L-H transition increases significantly when RMP fields of sufficient amplitude are applied in the L-mode phase of the discharge. The multi-machine results also confirm that a broad region in the edge pedestal with overlap of the vacuum magnetic islands from the RMP is not, by itself, sufficient to assure suppression of Type-I ELMs in H-mode plasmas. Using upgrades to the internal coil systems under construction or planned in several devices, future experiments, including joint experiments under the auspices of the ITPA, are expected to provide the essential physics understanding needed to project RMP results with confidence to ITER.

This work was supported in part by the US Department of Energy under DE-AC52-07NA27344, DE-AC05-00OR22725, DE-FC02-04ER54698, and DE-AC02-09CH11466,

and in part by EURATOM within the framework of the European Fusion Development Agreement. Views and opinions expressed herein do not necessarily reflect those of the European Commission. * See Appendix of F. Romanelli et al., paper OV/1-3, this conference

References

[1] EVANS T.E., *et al.,* Phys. Rev. Lett. **92** (2004) 235003
[2] BURRELL K.H., *et al.,* Plasma Phys. Control. Fusion **47** (2005) B37
[3] EVANS T.E., *et al.,* Nucl. Fusion **45** (2005) 595
[4] MOYER, R.A., *et al.,* Phys. Plasmas **12** (2005) 056119
[5] EVANS, T.E., *et al.,* Nature Phys. **2** (2006) 419
[6] EVANS, T.E., *et al.,* Phys. Plasmas **13** (2006) 056121
[7] EVANS, T.E., *et al.*, Nucl. Fusion **48** (2008) 024002
[8] FENSTERMACHER, M.E., *et al.,* Phys. Plasmas **15** (2008) 056122
[9] FENSTERMACHER, M.E., *et al.*, Nucl. Fusion **48** (2008) 122001
[10] UNTERBERG, E.A., *et al.,* J. Nucl Mater. **390–391** (2009) 486
[11] FENSTERMACHER, M.E., *et al.,* J. Nucl. Mater. **390–391** (2009) 793
[12] SCHMITZ. O., *et al.*, Phys. Rev. Lett. **103** (2009) 165005
[13] SCHMITZ, O., *et al.*, J. Nucl. Mater. **390-391** (2009) 299
[14] JAKUBOWSKI, M.W., *et al.,* Nucl. Fusion **49** (2009) 095013
[15] ORLOV, D., *et al.*, Nucl. Fusion **50** (2010) 034010
[16] HUDSON, B., *et al.,* Nucl. Fusion **50** (2010) 064005
[17] JAKUBOWSKI, M.W., *et al.*, accepted for publication in J. Nucl. Mater. (2011).
[18] LIANG, Y, *et al.,* Phys. Rev. Lett. **98** (2007) 265004
[19] KOSLOWSKI, H.R., *et al.,* Proc. 34th EPS Conf. on Plasma Physics, Warsaw, Poland, 2007, Vol. 31F (ECA) P-5.135 http://epsppd.epfl.ch/Warsaw/pdf/P5 135.pdf
[20] LIANG Y., Plasma Phys. Control. Fusion **49** (2007) B581
[21] ALFIER, A., *et al.,* Nucl. Fusion **48** (2008) 115006
[22] LIANG, Y., *et al.,* J. Nucl. Mater. **390-391** (2009) 733
[23] LIANG, Y., *et al.*, Nucl. Fusion **50** (2010) 025013
[24] LIANG, Y., *et al.,* accepted for publication in Plasma and Fusion Research (2010)
[25] LIANG, Y., *et al.,* Phys. Rev. Lett., **105** (2010) 065001
[26] KIRK, A., *et al.*, Nucl. Fusion **50** (2010) 034008
[27] NARDON, E. *et al.,* Plasma Phys. Control. Fusion **51** (2009) 124010
[28] KIRK, A., *et al.*, accepted for publication in J. Nucl. Mater. (2011).
[29] CANIK, J.M., *et al.*, Phys. Rev. Lett. **104** (2010) 045001
[30] CANIK, J.M., *et al.*, Nucl. Fusion **50** (2010) 034012
[31] SCHMITZ, O., *et al.*, Nucl. Fusion **48** (2008) 024009
[32] SCHMITZ, O., *et al.*, Plasma Phys. Control. Fusion **50** (2008) 124029
[33] UNTERBERG, B., J. Nucl. Mater. **390–391** (2009) 351
[34] MORI, M., *et al.*, Proc. 14th IAEA Conf. Plasma Phys. Control. Fusion *(*IAEA*,* Vienna, 1993) Vol. 2, p. 567
[35] SUTTROP, W., *et al.*, Fusion Eng. and Design **84** (2009) 290
[36] CAHYNA, P., *et al.*, Nucl. Fusion **49** (2009) 055024
[37] ITER Physics Basis Editors, Nucl. Fusion **47** (2007) S1.
[38] LOARTE, A., *et al.*, ITR/1-4 this conference
[39] SOLOMON, W.M., GAROFALO, A.M., private communication (2010)
[40] SCHMITZ, O., *et al.*, EXP/P3-30 this conference
[41] CHIRIKOV, B.V., Phys. Report **52** (1979)
[42] SCHAFFER, M. J., *et al.,* Nucl. Fusion **48** (2008) 024004
[43] GOHIL, P., *et al.*, EXC/2-4Ra this conference
[44] BECOULET, M., *et al.,* Nucl. Fusion **48** (2008) 024003
[45] LOWRY, C., Bull. Am. Phys. Soc. **54** (2009) 329
[46] NSTX Research 5-Year Plan for 2009-13, http://nstx.pppl.gov/fiveyearplan.html
[47] Rossel, J.X. *et al.*, Plasma Phys. Control. Fusion **52** (2010) 035006
[48] FUJITA, T. *et al*. Nucl. Fusion **47** (2007) 1512
[49] LEE, G.S. *et al.*, Nucl. Fusion **40** (2000) 575